The 12th Americas Conference on Wind Engineering (12ACWE)
Seattle, WA, USA, June 16-20, 2013

The 2006 Hanukkah Eve Storm and Associated Civil Infrastructure Damage in the Cascadia Region of the United States and Canada

Wolf Read [a], Dorothy Reed [b]

[a] *University of British Columbia, 2424 Main Mall, Vancouver, BC, Canada*
[b] *University of Washington, Campus Box 352700, Seattle, WA, USA*

ABSTRACT: A midlatitude cyclonic storm system bringing gust speeds ≥25 m s^{-1} and 24-hr rainfall ≥25 mm at many locations swept through the Pacific Northwest region of the US and Canada on 14-15 December 2006. The meteorological and climatological aspects of the storm are presented. Infrastructure damage data are then investigated, including the storm affects to trees, roads, bridges and with a strong focus on the power grid. Modeling by others using BC Hydro data that covers several years including the Hanukkah Eve Storm point to some correlation between rainfall intensity and electrical power interruption. The relationship between circuit failures and wind speed appears much stronger, with a magnitude above ~18 m s^{-1} appearing to have a high probability of outages. The data suggest that this type of storm system, bringing a combination of high wind and heavy rain, created conditions for significant damage in part due to reduced soil cohesion increasing tree vulnerability to wind stress, though extreme gust speeds in some regions were likely the dominant factor. Suggestions for system hardening are discussed.

KEYWORDS: Windstorm, rainstorm, infrastructure, damage, power grid, roads.

1 INTRODUCTION

The poor performance of civil infrastructure for natural hazards has been a focus in the wind engineering community in the US since the extensive destruction, some of it due to extreme wind loading, attributed to Hurricanes Katrina and Rita in 2005. Widespread storm-related damage is often due to a combination of high wind speeds with precipitation such as rain or snow, and flooding caused by rainfall or storm surge or a combination of the two. In this paper, we focus on winter storm losses caused by a combination of high wind speeds and extensive rainfall that created the conditions for flooding and soil saturation. The latter is conducive to tree root failure and rain-induced mudslides, which ultimately result in structural damage.

The infrastructure systems we investigate are roadways, bridges and electric power delivery systems. We note that a secondary effect of power outages is fatalities due to carbon monoxide poisoning because improper indoor heating systems are used during winter outages. Tree-related damage is both a part of so-called “green infrastructure” or environmental damage as well as a cause of damage so understanding their behavior is important in the region. Environmental damage is often rooted in land use changes. In the Pacific Northwest region, failed trees themselves often result in blocked roadways, downed power lines and building damage. Rapid recovery of these infrastructure systems post-event is a cornerstone of community resiliency.

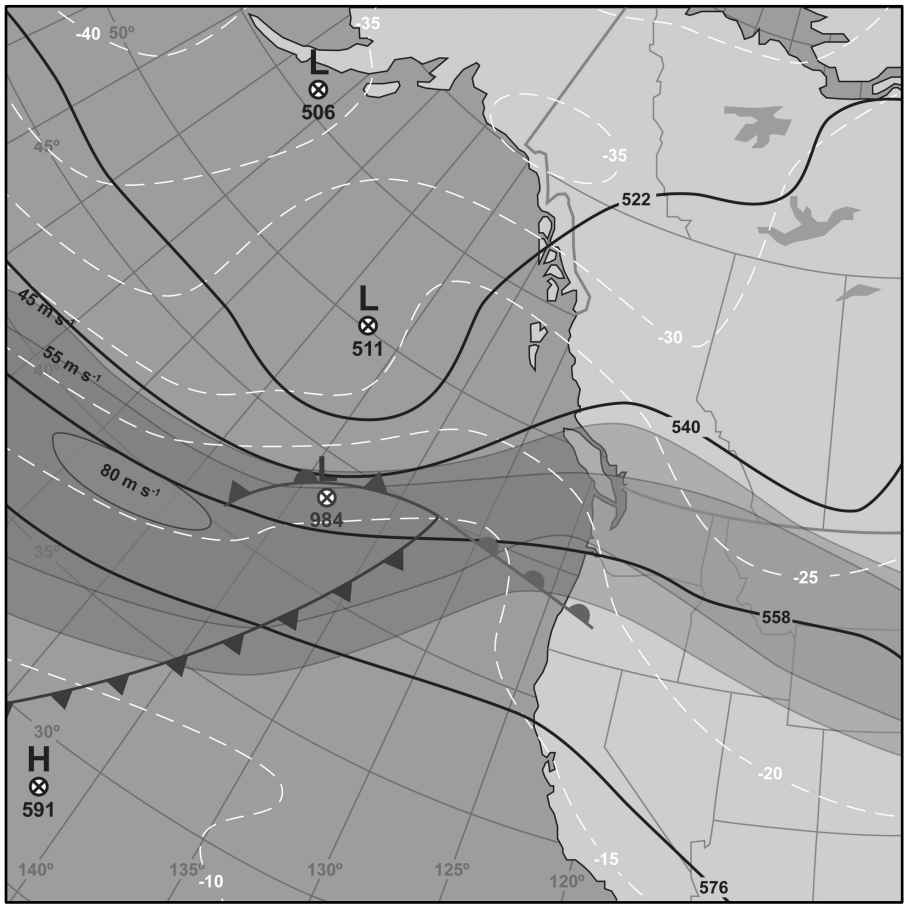

Figure 1. Synoptic analysis showing the rapid deepening phase of the Hanukkah Eve Storm. The maps depicts the 30 kPa jet stream core (shaded bands), with the surface low (circle an x-cross with 984) positioned in the left-exit region of a jet maximum. Shown for the 50 kPa level are the height lines in dm (heavy black), high and low centers (black circles with x-crosses) and isotherms (dashed white) in ºC.

We present results for the Hanukkah Eve Storm of 14-15 December 2006. Affecting communities from northern California (CA) in the US to southern British Columbia (BC), Canada, this storm event was a midlatitude cyclone with winds that occur roughly once in ten years, e.g. (1) and (2). We present the meteorological features of the storm in the next section before addressing the related infrastructure damage.

2 METEOROLOGICAL FEATURES OF THE STORM

2.1 *Synoptic and mesoscale analysis*

The Hanukkah Eve Storm, an extratropical wave cyclone (ETC), developed in classic fashion in a zone of baroclinicity under the left-exit region of an 80 m s^{-1} jet streak located over the Northeast Pacific Ocean. Figure 1 depicts the synoptic situation at 1200 UTC 14 December 2006, just as the low underwent explosive development. The map is a composite of charts produced by the National Center for Environmental Prediction (NCEP) and the Weather Prediction Center (WPC). The low tracked east-northeast to northeast

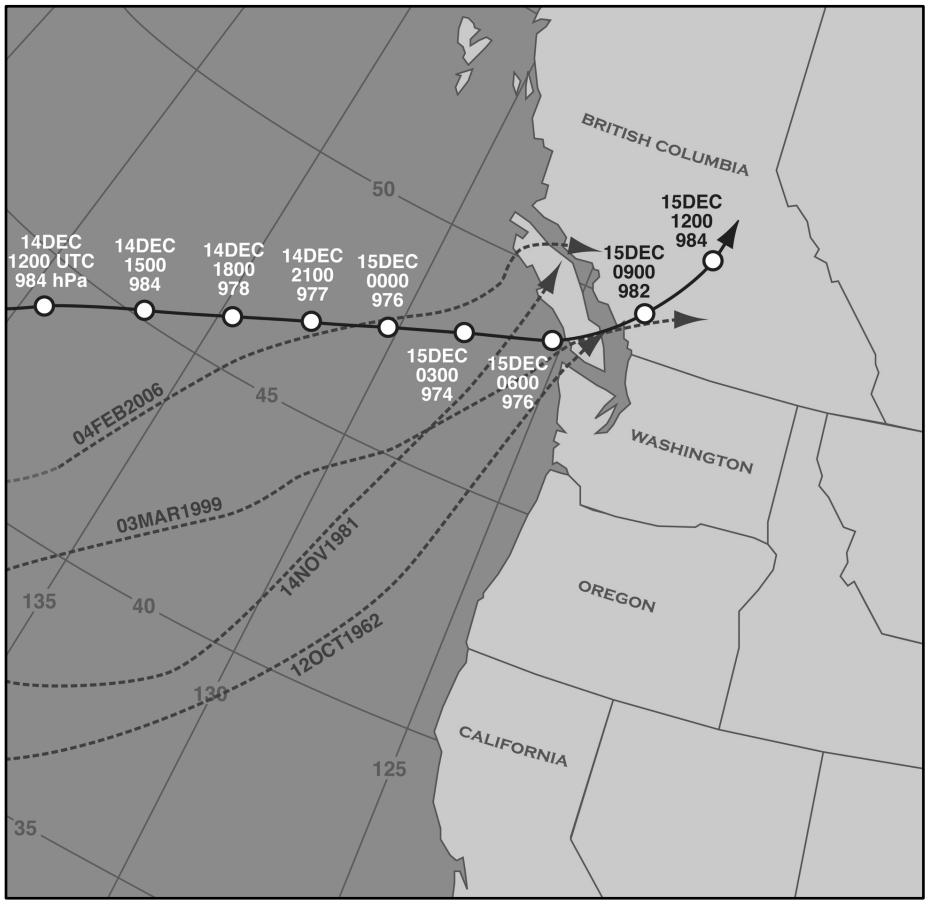

Figure 2. Track of the Hanukkah Eve Storm's center in the Pacific Northwest Region of North America, largely based on surface observation maps and satellite photos available from the Weather Prediction Center's archives, but with some reinterpretation including from the mesoscale analysis done here (Figure 3). Tracks of a few previous damaging storms are shown in the background.

toward the coastal waters of southwest BC, shown in Figure 2, deepening 9 hPa (12) h^{-1} to approximately 97.6 kPa by 0000 UTC 15 December. The 24-h deepening rate peaked at 20 hPa around 0600 UTC, a borderline case of "bomb cyclogenesis" given an average latitude of 43.8º N for the track suggesting a 19.2 hPa (24) h^{-1} cutoff for one Bergeron. Over the next 12 h, the surface cyclone tracked across southern Vancouver Island, filling as it moved away from upper support and encountered mountainous terrain, then recurved toward the north-northeast and skirted north of Vancouver, BC.

Figure 3, using available WPC surface maps and hourly and special observations from the National Climatic Data Center (NCDC), the Plymoth State Weather Center and Environment Canada (EC), shows a pair of mesoscale surface analyses separated by two hours during the period when the low center moved across southern Vancouver Island. As is depicted in the figure, the ETC appears to have brought inland at least three fronts: 1) a leading warm front, 2) a fairly vigorous cold front, and 3) a strong bent-back front. For well-developed and vigorous cyclones, the sharpest pressure gradients and associated wind speeds tend to be associated with the tip of the bent-back front (3), which is typically located approximately a few hundred kilometers southwest to south of the storm's center and often analyzed as an occlusion. The track of the cyclone on 14-15 December put the strongest part of the bent-back front over western Washington (WA) and southwest

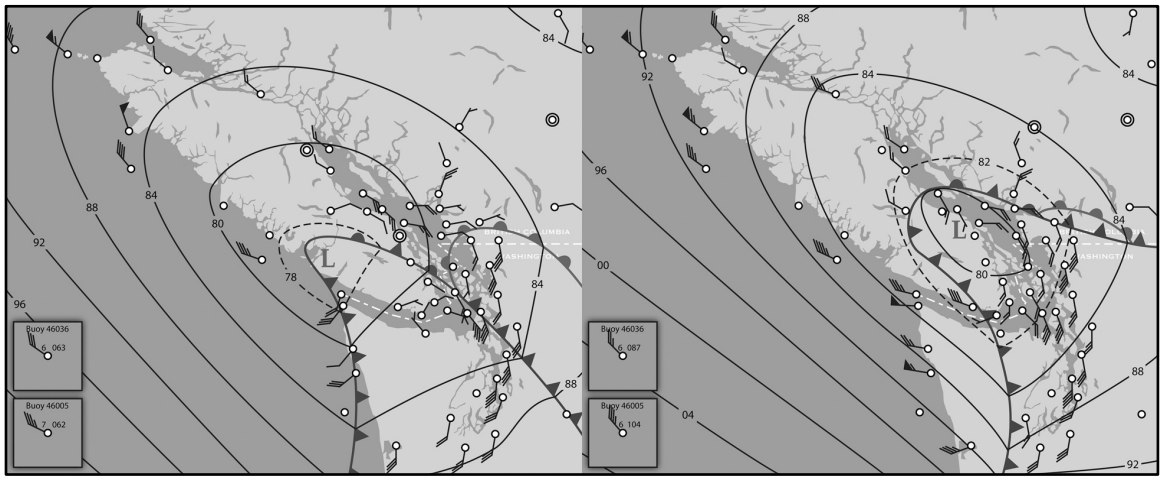

Figure 3. Mesoscale surface analysis showing the storm center tracking across southern Vancouver Island. Frame on the left depicts 0600 UTC 15 Dec 2006, with the next frame showing conditions two hours later. Wind speed indicators: ½ barb = 2.5 m s^{-1} (~5 kt), full barb 5.0 m s^{-1} (~10 kt) and pennant 25.0 m s^{-1} (~50 kt).

BC. Based on the surface weather response, including the presence of marked temperature drops with frontal passage, enhanced precipitation—in some places heavy—along the boundary, a sharp pressure surge and strong wind direction shifts to more westerly directions, it is not unreasonable to classify the bent-back front as a secondary cold front. Secondary cold fronts were recognized early in the development of the classic frontal cyclone model and appear to be generally overlooked today, perhaps due to tendency to put nearly every ETC into one particular template. Bjerknes and Solberg state (4): "It may happen, however, that one of the secondary cold fronts has a temperature and wind contrast much greater than that of the foremost boundary of the cold air. All air contained between the warm front and the strong secondary cold front may then act as a single large warm sector." Something akin to this appears to have happened during the Hanukkah Eve Storm. The highest winds during the windstorm, especially inland, occurred near this wraparound band (5), here analyzed as a secondary cold front.

2.2 *Wind magnitude*

For a given observation site, proximity to the cyclone's center tended to determine which of the three fronts produced the highest wind speeds and therefore the timing and extremity of the storm's peak gust. In western Oregon (OR), some stations reported their maximum gusts, roughly out of 180º to 200º, in the warm advection field post warm-front, generally around 1600 LST (LST +8 h = UTC) on 14 December. Another group of OR stations recorded their peak gusts, roughly out of 210º to 230º, with the passage of the leading cold front, around 2000. Further north, in WA and southwest BC, peak gusts were generally associated with the passage of the storm's bent-back or secondary cold front, which swept through the area just after midnight on 15 December. These winds, roughly out of 230º to 270º, sharply exceeded the already strong values recorded from the leading warm and cold front. Some exceptions exist to the above set of generalizations, likely because of terrain interaction. For instance, Bellingham (KBLI) experienced its highest gusts in a vigorous south-southeasterly gale just ahead of the secondary cold front, at 2349.

Table 1. Speed, direction and timing of peak gusts for the Hanukkah Eve Storm.

Location	5-sec gust (m s^{-1})	Direction (°)	Time (PST)
Arcata ASOS	16.1	210	2032
Cape Arago C-MAN	43.4	189	1636
Newport C-MAN	35.4	203	1636
Astoria ASOS	30.9	200	1534
Hoquiam ASOS	26.4	170	1915
Destruction Island C-MAN	35.9	195	1850
Quillayute ASOS	26.4	290	0015
Tatoosh Island C-MAN	35.1	274	0150
Medford ASOS	21.0	200	1501
Eugene ASOS	24.2	250	1930
Salem ASOS	23.7	220	1937
Portland ASOS	23.7	220	2007
Olympia ASOS	23.7	190	2353
Sea-Tac ASOS	30.9	220	0044
West Point C-MAN	31.6	196	0121
Smith Island C-MAN	33.8	254	0302
Victoria Gonzales Heights CON	34.0	260	0300
Victoria Intl EC CON	18.3	270	0400
Bellingham ASOS	24.6	160	2349
Vancouver Intl CON	26.4	290	0300

At the time of the windstorm, the National Weather Service's (NWS) Automated Surface Observation Stations (ASOS) recorded 5-sec average gust values on cup-based Belfort 2000 anemometers with some sonic systems being tested at a few locations. Environment Canada's gust records, for the observing sites used here, were a 5-sec vector average taken on cup-based 78D anemometers (6). Table 1 lists the available peak gust measurements for the storm. Figure 4 shows the location of most of the weather stations cited in Table 1. Figure 5 depicts the peak gusts for a broader selection of stations in western WA and southwest BC along with a more detailed look at the storm track. Five-sec gust readings, due to the relatively long averaging period, are generally lower than the older "instant gust" observations before the inception of ASOS (~pre-1996), perhaps by a factor of 1.1 (7). A running 3-sec average on the new Vaisalia 425 sonic anemometers implemented at NWS sites is thought to better equate the instantaneous speed on the older cup anemometers where the inertial response tends to smooth sudden spikes in wind speed to some degree. Gust readings in the table that exceed about 25 m s^{-1} represent a potentially very damaging storm. The 31 m s^{-1} recorded at the Sea-Tac Airport (KSEA), when adjusted for the averaging period, may indicate the highest instantaneous wind gust on record for this location.

Though ASOS stations typically have power backups, local communications systems can be shut down by electrical outages with resulting data loss. Due to the widespread electrical service interruption caused by the storm, data were lost at some critical stations located in the storm's primary damage path. These include Hoquiam (KHQM) where the last reliable transmission occurred at 2322 LST on 14 December; Shelton (KSHN), which ceased reporting regularly after 2353; and Olympia (KOLM), which ceased reporting after 2354. Other stations in the vicinity that were out of operation for reasons outside of the Hanukkah Eve Storm, perhaps due to a strong frontal system that swept through on 13 December, include Bremerton (KPWT) and the Jefferson Ridge RAWS sites (JEFW1). Despite the fact that data can be recovered from ASOS stations

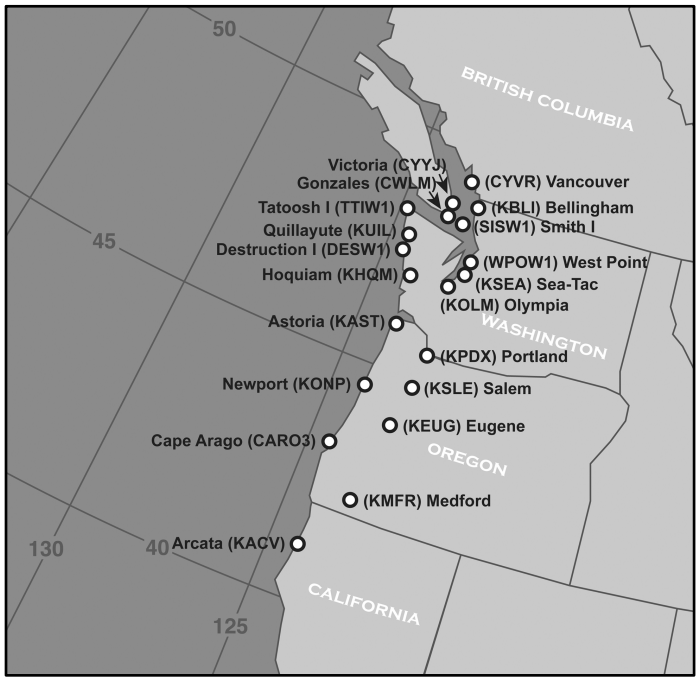

Figure 4. Locations of key official weather stations used in this paper.

post-transmission failure, there appears to have been little attempt to do so, as the datasets remain incomplete in the available NCDC DS3505 archives. In the case of KHQM, the station may have experienced damage, as the reporting of some variables such as altimeter and sea-level pressure continued during the outage period.

Data loss also occurred at KSEA, but this station continued to report nominally until 0225 LST, well after the primary wind strike from the secondary cold front. Figure 6 depicts the 1-min records of 5-sec gusts and sea-level pressures at KSEA up to the moment of data loss. Although wind direction is not shown in this figure, we note that the two highest 5-sec gusts of the storm, 31 m s^{-1} and 30 m s^{-1} occurred at 0044 and 0059, respectively, during a wind-shift phase from about 195º to 230º between 0000 to 0059. Barometric pressure jumped from 987.9 hPa at 0041 to 990.2 hPa at 0059 and would rapidly climb another 6.6 hPa over the next hour. The nearby National Data Buoy Center (NDBC) station at West Point (WPOW1) recorded a maximum gust of 29.6 m s^{-1} out of 179º at 0014 and 31.6 m s^{-1} out of 196º at 0121 which is a close fit in timing to the KSEA maximums. Quillayute (KUIL), a coastal location that transmitted a nearly complete wind record for the storm, reported a maximum gust of 26.4 m s^{-1} out of 290º at 0015. Destruction Island (DESW1) reported a peak gust of 35.9 m s^{-1} out of 195º at 1850, most likely associated with the leading cold front; but peak 2-min average winds occurred much later, with a speed of 29.7 m s^{-1} out of 282º at 0020 (gust 35.0 m s^{-1} out of 286º at 0035). Examination of data from RAWS sites also supports the timeline: The secondary cold front reached Black Knob (BKBW1) between 2230 and 2330, marked by a wind shift from SSW to NNW. Ten-minute average winds, on a 3-cup sensor at 6.1 m height (the standard for all the RAWS stations used here), reached 15.2 m s^{-1} out of the NW by 0130. At BKBW1, the storm peak of 15.4 m s^{-1} occurred out of the SSW at 2030, just after the leading cold front. At Humptullips (HUFW1), further inland and at an elevation of 730 m on a well-exposed ridge-top in the southern Olympic Mountains, the bent-back front swept through between 2255 and 2355, bringing maximum winds of 29.3 m s^{-1} out

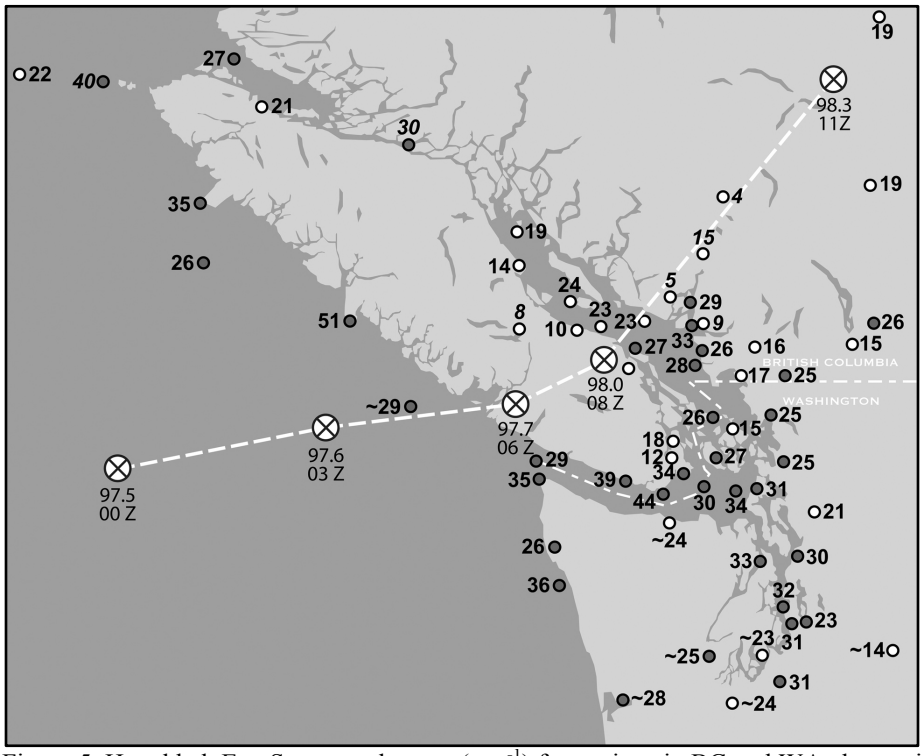

Figure 5. Hanukkah Eve Storm peak gusts (m s^{-1}) for stations in BC and WA along with storm track and estimated central pressure (kPa). Gust values in italics are estimated from peak wind via a 1.3 gust factor. Values with a tilde (~) are the highest available from stations the experienced significant data loss during the storm. Stations denoted in dark gray had gusts of ≥24.7 m s^{-1} (48 kt), rounded to the nearest whole number = ≥25 m s^{-1}. This is the approximate threshold U.S. NWS high-wind criteria (25.7 m s^{-1}, or 50 kt).

of the WSW by 0155. Across the Puget Sound Lowlands, at Enumclaw (ENCW1), the secondary cold front arrived by 0105 and brought peak winds of 18.0 m s^{-1} out of the SSW at this time.

The data from the above seven stations clearly indicate the arrival of the peak winds associated with the secondary cold front between 0000 and 0100 throughout much of the Olympic Peninsula and Puget Lowlands. These maximums appear to be associated with a sharp pressure gradient that moved in behind the bent-back front, evident in Fig. 3. The steep gradient resulted in strong pressure surges that mark progress of the bent-back front through the WA interior, as shown in Figure 7. Therefore, it appears that the final report times at the three stations with data-loss occurred just before the arrival of the strongest winds associated with the secondary cold front. Given the speed and direction of the cyclone, the timing of this extreme wind strike at KOLM and KSHN was perhaps between 0000 and 0030. At KHQM maximum gusts probably occurred between the last report at 2322 and 0000. Peak gusts were likely significantly higher at these locations than indicated in the available data, and were perhaps comparable to the 30 m s^{-1} recorded at KSEA and WPOW1.

2.2.1 *Climatological assessment of peak wind magnitude*

Available Seattle-area peak gust data for selected strong windstorms going back to 1962 are presented in Table 2. The table is divided into two sections due to a change in gust records with the commissioning of ASOS stations in the Pacific Northwest. Instant peak gust data recorded before the implementation of ASOS have been adjusted downward to

Table 2. Peak 5-second gusts for significant Seattle-Area windstorms, 1962-2006, in m s^{-1}. Values in italics are gust estimates based on the peak fastest mile value. The station name should be considered representative of the given location. To incorporate as much gust data as possible over a time period where stations were sometimes being moved and/or decommissioned, records for different, but close-proximity, stations may be present in a given column. "Seattle City" is represented by the University of WA ATG (2000-2006), City Office (1979 and 1983), Weather Service Forecast Office (1981) and the Naval Station at Sand Point (1962-1964). Tacoma data are usually from McChord Air Force Base, but sometimes are from the Narrows Airport (1981-1983).

Event	Tacoma	Sea-Tac Airport	Renton Airport	Boeing Field	West Point	Seattle City	Everett Paine	Average
ASOS-Era Storms (5-sec gust in m s^{-1})								
15 December 2006	31	31	23	25	31	25	30	28
04 February 2006	21	21	20	21	30	21	23	22
01 January 2006	18	22	18	18	24	18	20	20
25 December 2005	18	17	17	16	21	16	21	18
27 December 2002	23	23	22	21	26	25	26	24
16 January 2000	27	23	24	24	31	25	27	26
03 March 1999	25	27	23	23	30		26	26
Pre-ASOS Storms (Instant gust is adjusted to 5-second value in m s^{-1})								
12 December 1995	20	23	n/a	18	29	n/a	22	22
20 January 1993	23	24	28	26	23	n/a	25	25
24 November 1983	17	23	24	20	n/a	*21*	23	22
14 November 1981	17	25	26	17	n/a	24	20	22
13 February 1979	20	23	20	18	n/a	*23*		21
26 March 1971	21	23	22	17	n/a	n/a	21	21
19 January 1964	22	24	22	18	n/a	21	18	21
12 October 1962	33	22	38	25	n/a	25	30	29

reflect the 5-second gust measured by the newer stations using a factor of 1.19. With an average peak gust of 28 m s^{-1} (range 23-31 m s^{-1}), the Hanukkah Eve windstorm outclasses the strong 26 m s^{-1} values for the 16 January 2000 (range 23-31 m s^{-1}) and 3 March 1999 (range 23-30 m s^{-1}) events. These storms caused significant damage in Seattle, including the closure of key floating bridge spans across Lake Washington. With a 25 m s^{-1} peak gust average (range 23-28 m s^{-1}), the Inaugural Day Storm of 1993, remembered for causing widespread destruction throughout the Seattle area, was not as powerful as the 2006 event. Over 44 years of weather records have to be spanned to locate a stronger event than the Hanukkah Eve Storm: The 12 October 1962 gale had a Seattle-area peak-gust average of 29 m s^{-1} (range 22-38 m s^{-1}).

On a region-wide basis, the Hanukkah Eve Storm was likely the strongest since an intense 953 hPa low moved across the Olympic Peninsula on 12 December 1995. Table 3 shows peak gust data from Pacific Northwest windstorms for a representative sample of ASOS stations going back to the 1995 storm event. In this comparison, the Hanukkah Eve Storm's gusts were equal to or just slightly stronger than the 16 January 2000 and 3 March 1999 storms. When the average peak gust is taken to a 0.1 m s^{-1} resolution, the 2000 storm averages 23.5 m s^{-1}, and the 2006 event, 24.2 m s^{-1}; given that 1-knot equals about 0.5 m s^{-1}, this difference is within the resolution of the recording systems employed by the NWS and is considered credible. With an average of 24.9 m s^{-1}, the 12 Dec 1995 cyclone had slightly faster winds overall than the Hanukkah Eve Storm.

Table 3: Peak 5-second gusts for all significant and a few selected typical Pacific Northwest storms, 1995-2006, in m s^{-1}. The wind records at OTH and OLM during the 14-15 December 2006 windstorm are incomplete.

Event	ACV	OTH	AST	UIL	MFR	EUG	SLE	PDX	OLM	SEA	BLI	Average
14 December 2006	16	21	31	26	21	24	24	24	24	31	25	24
04 February 2006	17	23	26	24	14	21	17	20	19	21	28	21
01 January 2006	20	19	21	23	16	18	20	20	20	22	24	20
25 December 2005	16	25	24	16	13	17	16	21	18	17	21	19
29 January 2004	16	21	21	21	21	17	20	18	17	18	19	19
05 December 2003	11	20	22	16	7	13	15	14	17	14	19	15
27 December 2002	14	27	26	14	13	17	17	17	18	23	10	18
07 February 2002	17	24	15	4	16	31	14	14	7	9	9	15
13 December 2001	19	26	22	22	12	16	20	17	18	18	18	19
16 January 2000	21	23	30	20	17	17	27	26	24	23	30	24
03 March 1999	18	22	30	25	17	23	21	23	21	27	28	23
06 February 1999	15	24	25	14	18	21	19	18	17	20	18	19
05 February 1999	7	23	22	19	6	16	17	19	17	18	25	17
01 January 1997	21	29	25	21	11	20	18	23	21	17	25	21
12 December 1995	22	32	28	23	20	22	26	28	21	23	29	25

2.3 *Precipitation magnitude*

Many stations that were subjected to high wind gusts also experienced heavy rain during the storm. Based on precipitable water analysis available every 12-h from NCEP, the Hanukkah Eve storm brought a moisture plume with values in the range of 19-24 mm (0.75-0.95") to western OR and WA between 1200-0000 UTC on 14-15 December. Though quite moist, other storms of history, including atmospheric river events, have had precipitable water values upwards of twice this amount. Nevertheless, the NCDC archives indicate that a number of daily 24-h rainfall maximums were established in WA and OR on 14 December, with 38 stations setting new extremes for the day and five tying records. Figure 8 uses output, in a modified form, from the NCEP Environment Modeling Center (EMC) stage-IV precipitation estimate for the 24-h ending 1200 UTC 15 Dec 2006. Unfortunately, this output does not include Southwest BC. From the Willamette Valley northward, lowland areas generally received 25 mm or more of rain, with some locations receiving nearly 50 mm. In the uplands, totals above 75 mm were common and in some places, especially in the Olympics, values reached approximately 150 mm. Figure 9 shows the 24-hour totals for ten key weather stations within the storm's strike zone for 13-15 December 2006. Values on 14 December 2006 clearly stand out among the three days.

Rainfall rates were particularly intense within a line of thunderstorms that developed along the warm front as it moved into the Puget Lowlands. In the hour ending 1753, KSEA recorded 7.9 mm of rain accompanied by occasional lightning and gale-force wind gusts. Heavier precipitation amounts were reported within the Seattle city limits, including 23.6 mm in the hour ending 1700 at the NOAA Weather Forecast Office (8). Boeing Field (KBFI) reported 48.8 mm in 24-h on 14 December, breaking the previ

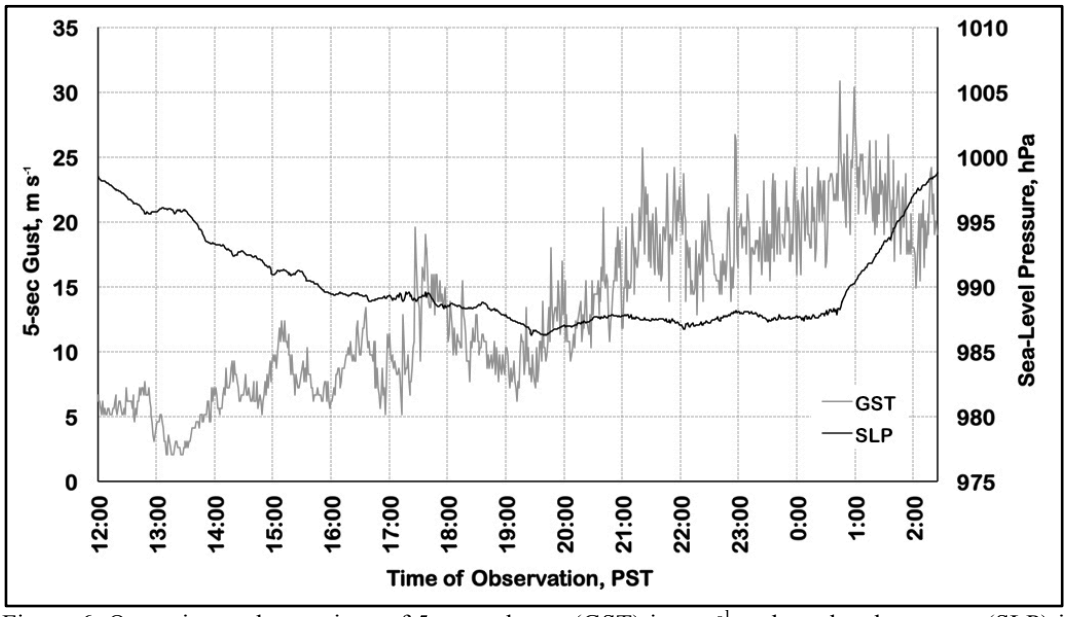

Figure 6. One-minute observations of 5-second gust (GST) in m s^{-1} and sea-level pressure (SLP) in hPa at the Seattle-Tacoma International Airport. Data are from the National Climatic Data Center.

ous daily record by 25.4 mm. Emphasizing the significance of this Seattle rain event, more than two hundred residents made claims against the city for flood damage caused by the overloaded storm-water and sewage system (9). Figure 10 portrays the cumulative rainfall at Sea-Tac Airport from the time period 1200 PST to 0224 PST on 14-15 December 2006. The gust record is included in the figure for reference. A burst of extremely heavy rain arrived around 1700, during a broader period of intense precipitation that occurred between 1615 and 1745. The first gale-force gusts of the storm immediately followed the heaviest precipitation. The downpour combined with wind surge clearly marks the arrival of the storm's leading cold front.

The relatively heavy amounts of rain during the Hanukkah Eve Storm fell after many weeks of moist Pacific storms. November 2006 especially proved extremely wet for parts of the region, as exemplified by stations that received their all-time highest one-month rainfall totals on record such as Sea-Tac with 397.0 mm; Hoquiam with 543.1 mm; and Stampede Pass with 712.0 mm (10). An estimation of the Nov 2006 precipitation anomaly, shows much of the US Pacific Northwest with > 170% of normal (11). Given the additional moisture provided by the Hanukkah Eve Storm and other strong ETCs during the preceding week, soils throughout the strike zone were saturated when the strongest wind arrived. Waterlogged soils have weaker cohesion and shear strength (12). Under these conditions during high winds, trees may be more prone to toppling from root failure (13, 14). Electric utility pole configurations might also be at higher risk.

3 INVESTIGATION OF DAMAGE

3.1 *Tree damage*

Widespread windthrow, including some swathing events where large contiguous areas of trees were toppled, occurred throughout a broad area including western OR, WA and

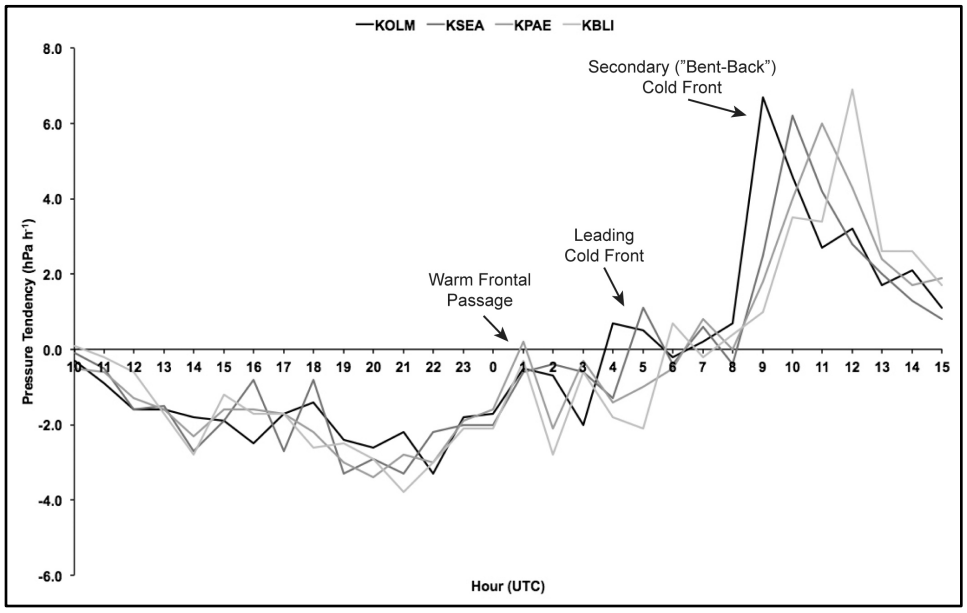

Figure 7. One hour pressure tendencies at four key stations in the WA interior. Passage of the three fronts associated with the Hanukkah Eve Storm are evident in changes from strongly negative to weakly negative and positive values. The secondary cold front produced a strong pressure surge at all four stations, reflecting a strong pressure gradient behind the bent-back front, and also a progressive storm.

southwest BC. One of the authors (Read) while surveying storm damage from Corvallis, OR, to Seattle, WA, observed a high percentage of root-failures, suggesting weakened rootholds due to high water content in the soil, in wind-toppled trees, with stem-breaks becoming increasingly common from about Olympia, WA, northward. About 40,000 m^3 of timber were lost on state lands in Clatsop County, OR (15). Large areas of windthrow also occurred on WA State lands, including the Capitol Forest (16). The South Puget Sound Department of Natural Resources planning unit appeared to have the most tree damage, with some windthrow in coastal sections (17). In Vancouver, BC, historic Stanley Park experienced a frequency of tree failure comparable to the Columbus Day Storm of 1962, with the loss of thousands of trees in large swaths (18). Heavy tree damage continued in a relatively narrow line from Stanley Park down the Burrard Inlet to the vicinity of Deep Cove.

3.2 *Transportation systems including roadway and bridge closures*

The Washington State Department of Transportation (WSDOT) placed staff and equipment at key transportation points in the state in preparation for the storm. Road closure first occurred near downtown Seattle on 14 December 2006 at 1700 PST when standing water covered multiple lanes on the primary freeway Interstate I-5 (19). More than 50 state highway closures were reported. We analyzed a spreadsheet provided by WSDOT that had data collected during the storm by bridge repair and maintenance staff of eighty-eight roadway closures along with time durations and the reason for closure. Of the roadways and bridges, the majority (67%) were closed due to fallen trees and rocks that blocked traffic. Downed power lines and flooding created 10 percent of the closures. Six percent of closures were due to high crosswinds. Finally, seventeen percent of the closures were due to mudslides, traffic light failures and car accidents that blocked traffic. In Vancouver, BC, due to the failure of over 100 stoplights, some from loss of electrical

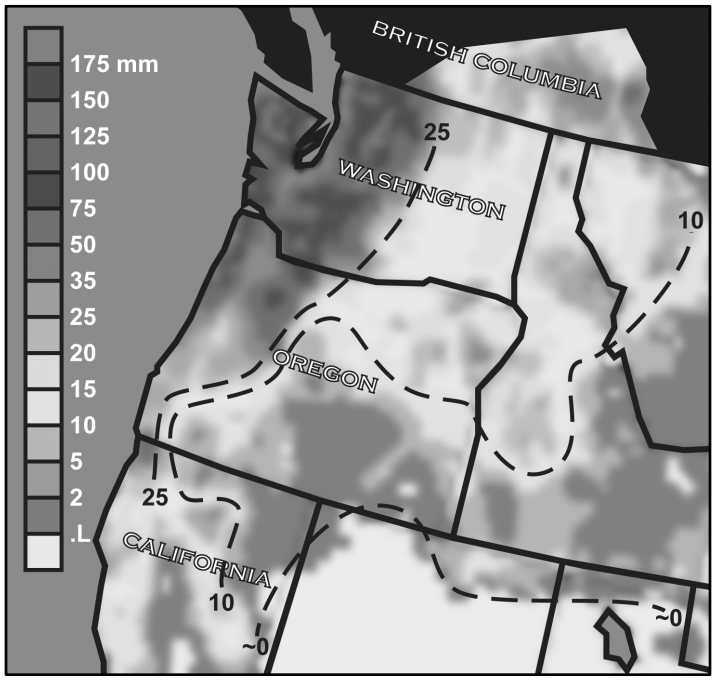

Figure 8. Modified output from the NCEP/EMC Stage-IV (3-model) estimate of total precipitation (mm) in the 24 hours ending 1200 UTC 15 Dec 2006. Areas shaded in black were not included in this analysis. Due to poor grayscale reproduction quality, three isohyets in mm were added to help guide the eye in what was intended to be a color graphic.

service and others from damage due to wind, traffic became impeded during the morning commute on 15 December (20).

The Puget Sound region has several bridges that span waterways and most of these were closed for the duration of the storm, including the suspended-span Tacoma Narrows Bridge (19). In Vancouver, BC, the Lions Gate Bridge had to be shut down during the morning commute due to numerous trees down on the Stanley Park Causeway, the trunk connecting the bridge to downtown (20). Indeed at least three key arteries in the metro area were shut down. Power outages also disrupted Vancouver's electric SkyTrain commuter rail service, and a train on one line hit a tree that had fallen across the tracks, causing damage to the vehicle and delay of service.

Ferry lines are an important part of the city transportation grid. Three ferry runs in the Puget Sound region were affected during the storm (19). A few BC Ferries sailings were cancelled, and SeaBus operations in Vancouver were slowed due to a barge, carried by the wind, colliding with one of the berths (20). The overnight timing of the storm, with peak winds between 2000 and 0400 LST when mass transit systems are at lower capacities, probably explains why a much larger disruption of ferry systems did not occur (e.g. cancellation of numerous sailings).

Transportation systems play an important role in the recovery of a community post-storm. Communication of the status of the transportation grid to other infrastructure systems personnel is critical: Power crews need access to downed power lines and other regions where roads are blocked. Commuters need real-time information in order to avoid closed or congested roadways. Recovery efforts for transportation therefore include a strong communications role.

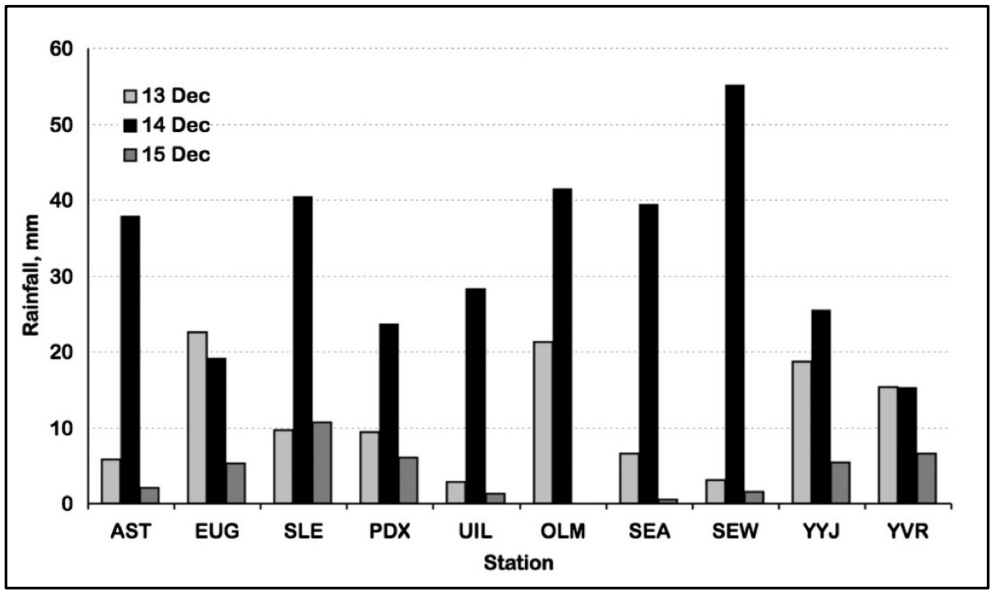

Figure 9. Daily rainfall totals for selected stations in the Hanukkah Eve Storm's strike zone. Data from the National Weather Service Seattle and Portland forecast offices and Environment Canada.

3.3 *Power outages*

Power outages were extensive. In WA State, over 1.5 million customers lost electrical service during the storm. Most of those affected were in the Puget Sound Energy service area. Over 700,000 customers of Puget Sound Energy lost power in the storm; 159 sub-stations were impacted and 85 transmission lines were out (21). With approximately 250,000 customers affected, BC Hydro appears to have experienced the largest disruption of its electrical infrastructure since the great 1962 Columbus Day Storm when at least 40% of the customers in the Lower Mainland and Victoria service areas had their power cut (22, 23). After the Hanukkah Eve Storm, service teams faced challenges in the resto-ration of power delivery systems because fallen trees and storm debris blocked many streets. In the case of BC Hydro, crews nearly became overwhelmed because the wind-storm closely followed two others during the same week, one of which disrupted power to 190,000 customers on 11 December (24, 25).

3.3.1 *Civil engineering outage analysis*

The civil engineering community has traditionally employed a function $Q(t)$ to denote the quality of service or operability of a system such as power delivery. It has been employed primarily to describe structural performance over time following earthquakes, e.g. (26), but it is equally applicable to wind events. In equation form, the quality $Q(t)$ is

$$Q(t) = Q_\infty - (Q_\infty - Q_0)e^{-bt} \tag{1}$$

where Q_∞ is the capacity of the fully functioning structural system, Q_0 is the post-event capacity, b is a parameter derived empirically from restoration data following the event and t is time in days post-event.

It is convenient to characterize quality in percent where 100% represents a fully functioning system. Modifying the equation in this manner means dividing by Q_∞. For the systems under consideration in this paper, $Q(t)$ = 100% is fully operable (zero outages)

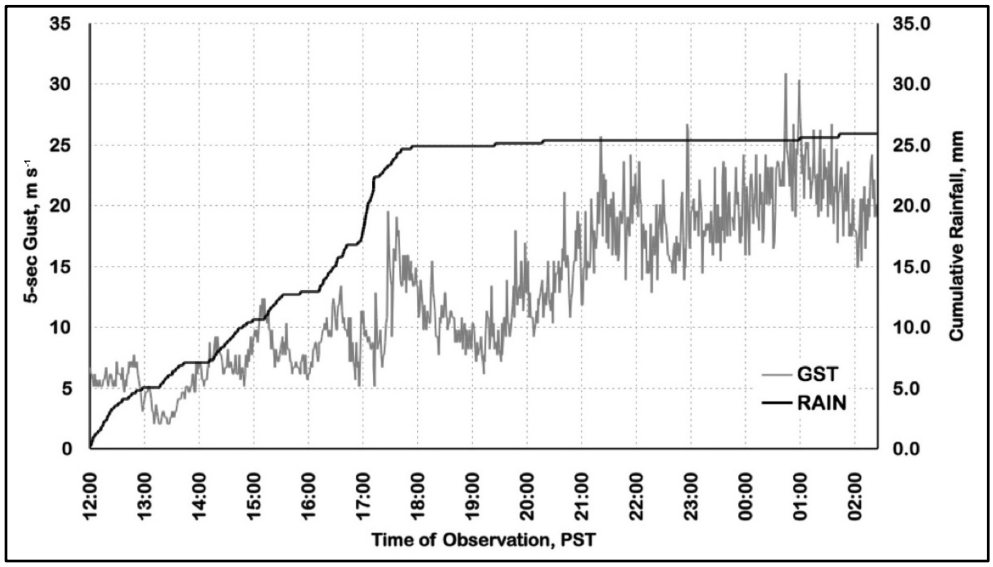

Figure 10. One-minute observations of cumulative rainfall in millimeters, with 5-second gust (GST) in m s^{-1} for reference, at the Seattle-Tacoma International Airport. Data from the National Climatic Data Center.

and 0% is inoperable (100% outages). Values between these two represent varying degrees of system operability.

Resilience R is a measure that may be calculated from the quality function as follows:

$$R[\%] = \frac{\int_{t_1}^{t_2} Q(t)dt}{100(t_2 - t_1)} \tag{2}$$

where t_1 and t_2 are the endpoints of the time interval under consideration.

Resilience is said to have other properties including *robustness*, *rapidity* and *resourcefulness* (26). We have plotted quality curves for several power companies affected in the Pacific Northwest including BC Hydro of Canada in Figure 11 using data obtained from the US Department of Energy Situation Reports (27). The figure shows that Puget Sound Energy (PSE) had a robustness of approximately twenty percent and Tacoma Power at thirty percent while BC Hydro was at eighty-five percent. Part of the difference is attributed to the location of the facilities. Only a small portion of BC Hydro was in the path of the storm relative to PSE and Tacoma Power.

Recovery may be compared through the use of the parameters in equation (1) for the $Q(t)$ function. Table 4 provides the values of the rapidity parameter b in equation (1) and the resilience R of equation (2) for each company as well as some goodness of fit information. It is noted that Puget Sound Energy was particularly hard hit by the storm as it had the least robustness, resilience and longest restoration time. In comparison, the parishes of Louisiana affected by Hurricane Katrina had a robustness of approximately 20%, a rapidity parameter of 0.05 for a forty-day recovery period, and a resilience of 68%.

3.3.2 *IEEE performance index analysis*

One of the industry standards for characterizing utility outages is the System Average Interruption Index, *SAIFI*, as defined by (28) as

$$SAIFI = \frac{\sum \text{Customer Interruptions}}{\text{Total Number of Customers}}$$

(3)

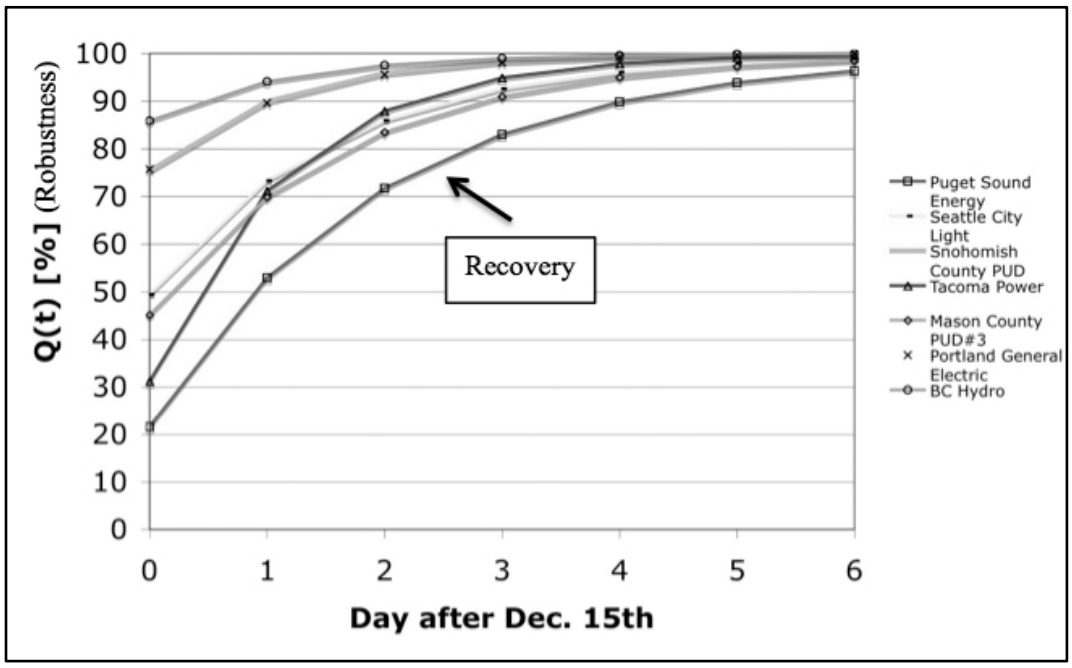

Figure 11. Quality *Q(t)* comparison for the power companies post 15 December.

For the Pacific Northwest, *SAIFI* is approximately 0.3 interruptions per year according to Seattle City Light (2002). *SAIFI* does not include "major" events when more than ten percent of all customers lose power. For major events, we use *STAIFI* as defined by (29) where the *SAIFI* value is evaluated for the duration of the storm. That is, the amount of outages for a storm is characterized in terms of the normal number of non-storm outages for the same location. For the Pacific Northwest data, the average *STAIFI* was 38 interruptions per year. In other words, if the interruption behavior during the storm were "distributed" across the year, it would result in 38 significant outages over that year as opposed to 0.3 interruptions per year, which is the normal non-storm value. In previous analyses of winter storms Reed (30) found that a normalized *STAIFI* designated as $STAIFI_n$, as defined by

$$STAIFI_n = \frac{STAIFI \text{ for the storm data in interruptions per year}}{SAIFI \text{ for the year the storm occurred in interruptions per year}} \tag{4}$$

was linearly related to a gust ratio; that is, the peak 5-second gust divided by the monthly peak gust for the year the storm occurred. We obtained a similar relationship as for the Hanukkah Eve data as $STAIFI_n = 135.2G^2$ where

$$G = \frac{\text{peak 5-second gust for the storm}}{\text{monthly peak 5-second gust at the same location}} \tag{5}$$

Unfortunately, this relationship did not have a very high goodness of fit (R^2 = 40%). We are currently investigating other functional relationships.

Table 4: Quality and resilience parameters.

Utility	Total Number of Customers in the System	Rapidity parameter "b" in equation (1)	Goodness of fit parameter R^2 [%]	Resilience in [%] in equation (2)
BC Hydro (2007)	1700000	0.88	99.4	97.1
Mason County PUD#3	31000	0.60	96.6	84.8
Portland General Hydro	680093	0.85	98.9	95
Puget Sound Energy	*893576*	*0.51*	*86*	*75*
Seattle City Light	336363	0.64	96.8	86.7
Snohomish County PUD	272829	0.89	94.1	94.9
Tacoma Power	145375	0.87	96.8	86.1

3.3.3 *Power grid fragilities*

In addition to quality curves and performance indices, civil engineers also employ the use of fragility functions to predict the wind speeds associated with various damage levels of the percentage of the entire stock of a structural type. Fragilities are defined as "the expected number of occurrences of a particular type of damage as a function of the loading parameter, such as wind speed or rainfall". In order to derive fragility curves for a structural type, geographical information system (GIS) data for the locations and amounts of structural damage and the weather parameters such as basic wind speed and rainfall are required. For the Hanukkah Eve event, we largely did not have accurate GIS data for the damage to trees, roadways or power delivery systems in the afflicted region, making a fragility analysis unfeasible at this time. BC Hydro did provide datasets for a study only indirectly related to this paper, namely a threshold analysis that is still underway, but this information only covers part of the region afflicted by the Hanukkah Eve Storm. Though clearly not impossible, data from agencies such as power companies can be difficult to obtain in part due to a fear of releasing information that could be tied to private individuals and also concerns about public perception of utility performance. In one case, an author could not access a public utility library without being an employee of the agency, and in another several queries about acquiring power outage data for specific storms were not even acknowledged. When data is released, sometimes there are significant restrictions on its use.

Despite the difficulties, some analysis has been done on the transmission grid for BC and the distribution network for the North Shore area of the Greater Vancouver Metro District (31). This study used the same BC Hydro dataset given to us. Tree-related outages affecting the North Shore distribution grid during 15 Oct 2005 to 15 Aug 2009, a time period that includes the Hanukkah Eve Storm, were compared to gridded numerical weather prediction (NWP) data including average hourly precipitation and wind speeds, topographic indicators including elevation and slope, and stand variables including tree height and age. Vegetation coverages were generally not available among many power line corridors, especially in urban settings, though stand characteristics were available in some locations. A logistic regression model relating outages to topographic exposure, tree height, and average hourly precipitation had a c-value of 0.62, suggesting some correlation with these three indicators. Another model using elevation, topographic exposure, a one-km gridded annual wind speed dataset from BC Hydro and the top-five wind

events from the four-km Canadian Mesoscale Community Compressibility Model (MC2) also returned a c-value of 0.62.

Taylor and Neale (32) employed a statistical method called "threshold analysis" (33) to ascertain the maximum gust and percentage above normal rainfall at which significant damage occurred to the BC Hydro. Using data for storms with significant outages from 2004 to 2007, they found for the Victoria, BC, area that maximum wind gusts of $\geq$70 km h^{-1} (19.4 m s^{-1}) and antecedent rainfall in excess of 10% of normal (presumably 1971-2000) to be useful thresholds for expecting outages. The advantage of this type of analysis is the ability to predict when widespread damage occurs due to the combination of heavy rain and high winds using a much smaller data set than with GIS analysis. The usefulness of this method is still under investigation by the writers for other storm data.

A preliminary analysis on the 2005-2009 BC Hydro dataset done by one of the authors (Read) for distribution circuits within a 50 km radius of the Vancouver International Airport, indicates that a 2-min wind speed threshold of roughly $\geq$65 km h^{-1} (~18 m s^{-1}) is almost always associated with at least one tree-related power outage (unpublished data).

We note that the Hanukkah Eve Storm far exceeded the above wind, gust and precipitation thresholds at many locations in western WA and southwest BC, indeed more than 50% in some instances. This indicates that the resulting damage should have been significant.

Models for the prediction power outages outside of the study area have been developed for regions in the United States and Canada. Much focus has been on eastern events, especially hurricanes and ice storms (13, 34, 35). These approaches may point the way for further modeling work on windstorms in the Cascade region; however, key differences in tree species, terrain type, the characteristics of Pacific ocean ETCs verses hurricanes and Eastern midlatitude cyclones, electric utilities and other factors limit the applicability of these studies specifically to an analysis of the Hanukkah Eve Storm. Other approaches, such as the Poisson regression and Bayesian network models described by Zhou *et al.* (36), which can incorporate a wide range of weather conditions, also appear to be a useful direction for future efforts at predicting electrical service interruption during high winds in the Pacific Northwest.

3.4 *Fatalities*

Thirteen deaths were attributed to the storm in the Puget Sound region according to Green *et al.* (37). Eight of those fatalities occurring in King County, WA, were due to smoke inhalation or carbon monoxide (CO) poisoning among families in their homes using improperly ventilated generators. Indeed an epidemic in CO poisoning totaling 259 cases occurred in the county between 15-24 Dec 2006, the most significant outbreak in US history (38). Many cases were non-fatal and most were apparently linked to the use of portable devices for home heating during the prolonged power outage associated with the storm. Fatal CO poisoning also occurred in Burnaby, BC (39). Although many public service announcements were made regarding the dangers of smoke inhalation and carbon monoxide poisoning, most of the families who died were immigrants who spoke little or no English. Other deaths occurred due to drowning and trees falling on occupied cars or trailers.

4 IMPLICATIONS FOR STORM HARDENING

Structural engineers achieve improved performance in buildings through enhancing redundancy and robustness. In terms of the Hanukkah Eve event, falling trees were a major factor in structural damage and roadway closure. Urban drainage conditions should be evaluated prior to the winter storm season in order to assess the vulnerability of buildings, roadways and power lines. Soil moisture is evaluated by the Climate Prediction Center (40). Perhaps such soil moisture information, in combination with analysis the performance of root anchorage for key species in local soil types, could be used to create an estimate of tree vulnerability. However, such an assessment may require monitoring soil moisture in near real-time and at fairly high spatial resolution as a storm can bring significant precipitation within short time spans and be focused on small regions. Land use guidelines may be useful in identifying more robust conditions for tree survival. Forest management practices, applied in critical areas, for tree and stand-level wind-firmness may reduce the risk of tree failure, e.g. (41).

For the power delivery system, enhanced structural redundancy and resilience at the network level appears to be appropriate. Clearly the repair and reconstruction of transmission lines and towers would be quicker in regions that are more conducive for crew access. The structural form of tower failure is another topic for examination. Newer tower forms such as cross-arm steel or concrete may exhibit greater ductile capacity to deform under loading. In addition, the ability of individual towers to "drop" lines may be useful at certain wind speeds in order to avoid a series-type line failure. Wooden towers and poles appeared to fail at or near the base in exposed regions. In these instances, geotechnical examination and tower base redesign should be considered. Use of geotextiles commonly applied to slope stability, e.g. (42) may be appropriate to strengthen the base support for selected poles. Geofibers to anchor tree root systems may also be a consideration. The large number of substations that sustained damage due to airborne debris and high winds suggests that more rugged designs for housing the electrical equipment be investigated.

5 SUMMARY AND CONCLUSIONS

The Hanukkah Eve storm was a so-called "ten year event" that caused much greater damage than its predecessor, the 1993 Inaugural Day Storm. Most of the damage was to the interdependent infrastructure systems such as the power delivery system and the transportation grid. Evidence of the interdependencies as described for hurricanes between power delivery and transportation, e.g. (43), is suggested by our results for this storm: Downed power lines and traffic light failures played a role in roadway closures while access to power lines was limited by closed roadways. Coordination between the two repair and recovery teams is important. Power outages can also create difficulties in the winter due to low temperatures. Air quality suffers during periods of extended outages due to smoke from fireplaces (44). The few deaths that occurred were primarily attributed to carbon monoxide poisoning or smoke inhalation. Investigations of the infrastructure damage are ongoing at the University of Washington.

We have examined the structural system damage to the power delivery infrastructure for the storm. The traditional IEEE performance index *SAIFI* has been estimated and restoration and quality have been investigated. Despite the limited data available we have the following preliminary conclusions.

- The consequences of tree-related damage suggest that additional investigations be undertaken to evaluate tree health and resilience in the Pacific Northwest.
- The IEEE-based performance index *STAIFI* may not be as useful for structural engineers in predicting damage as for utility companies to assess performance for electrical engineering considerations. Resilience measures are more descriptive for structural engineers as they may be used to characterize robustness and the rapidity of restoration. However, the performance index does implicitly indicate the level of resources employed in restoration and may ultimately be related to the resilience parameter of "resourcefulness" as employed in the model described by (Bruneau et al. 2003).

Finally, trees are a cherished part of the ecosystem in the Pacific Northwest yet their failure can trigger building damage, roadway closures and downed power lines. Patterns of failures in exposed stands and newly developed suburban regions suggest that further investigation of species behavior and land use regulations is warranted.

6 ACKNOWLEDGEMENTS

Students J. Lee, A. Loeffler, X. J. Mei and J. Perkizas at the University of Washington are acknowledged for their efforts in organizing the WSDOT bridge data. We thank BC Hydro, and the former sister agency BCTC, for supplying outage data, and providing funding for the preliminary analysis mentioned in this paper. We also thank the anonymous reviewers: their considered input helped strengthen this paper.

7 REFERENCES

1 C.F. Mass, How Unusual was the December 14-15th Windstorm? Presentation to the Utilities and Transportation Commission, Washington State, (2007).
2 W. Read, The December 14-15 2006 Windstorm, The Storm King: Some Historic Weather Events in the Pacific Northwest, Office of the Washington State Climatologist website, available at: http://www.climate.washington.edu/stormking/, last accessed on 10 Aug 2011, (2011).
3 W.J. Steenburgh and C. F. Mass, Interaction of an intense extratropical cyclone with coastal orography. Mon. Wea. Rev., 124 (1996) 1329-1352.
4 J. Bjerknes and H. Solberg, Life cycle of cyclones and the polar front theory of atmospheric circulation. Geofysiske Publikationer, 1 (1922) 3-18.
5 C.F. Mass and B. Dotson, Major extratropical cyclones of the Northwest United States: historical review, climatology, and synoptic environment. Mon. Wea. Rev., 138 (2010) 2499-2527.
6 Environment Canada, Manual of Surface Weather Observations, 7th Edition, Ammendment 18, Environment Canada, 2013, pp. 101-105.
7 Automated Surface Observation System (ASOS) Release Note Software Version – 2.7A Replacement Wind Sensor (Vaisala 425 Ice-Free Wind Sensor), Draft, US Department of Commerce, 2002.
8 NOAA Preliminary Local Storm Report, NWS, Seattle, WA, 1818 PST, 14 Dec 2006.
9 S.P. Chan, More than 200 claim city owes them for flooding, The Seattle Times, 20 Jan 2007.
10 Office of the Washington State Climatologist (OWSC), 2006 November Record Rainfall. Available from http://www.climate.washington.edu/events/2006NovRain.html, last accessed 07 May 2013.

11 PRISM Group, Precipitation Anomaly Nov 2006 Final Data. Available from http://www.prism.ORstate.edu/products/matrix.phtml?vartype=ppt_anom&view=maps&year0=2000, last accessed 29 Apr 2013.
12 R.J. Schaetzl, D.L. Johnson, S.F. Burns and T.W. Small. Tree uprooting: review of terminology, process, and environmental implications. Can. J. of For. Res., 19 (1989) 1-11.
13 S. Han, S.D. Guikema, S.M. Quiring, K. Lee, D. Rosowsky and R. A. Davidson, Estimating the spatial distribution of power outages during hurricanes in the Gulf Coast region, Reliab. Eng. & Syst. Saf., 94 (2009) 199-210.
14 K. Kamimura, K. Kitagawa, S. Saito, H. Yazawa, T. Kajikawa and H. Mizunaga, Root anchorage under the combined condition of wind pressure and intensive rainfall: tree-pulling experiments with controlled soil water content, 2nd International Conference Wind Effect on Trees, ed. H. Mayer, Self-publishing company of the Meteorological Institute, Albert-Ludwigs-University of Freiburg, Freiburg, Germany.
15 C. Profita, Timber Revenue Blows in After Storm, The Daily Astorian, 12 Sep 2007.
16 WA Department of Natural Resources, Forest Health Highlights in Washington-2007, Apr 2007.
17 W. Jaross, South Puget Sound Department of Natural Resources, personal communication, 18 Aug 2008.
18 S. Mitchell, Stanley Park's recovery, Branch Lines, 18 (2007) 1-8.
19 J. Himmel, T. Trepanier, C. Christopher and M. Coon, WSDOT December 06 Wind Storm Preparation, Response and Recovery Actions, Washington State Department of Transportation, 2007.
20 W. Boei, Commuter chaos on roads, transit, Vancouver Sun, 16 Dec 2006, B4.
21 S. McNeil, Puget Sound Energy: The Mid-December Storm. Presentation to the Utilities and Transportation Commission, WA State, 08 Feb 2007.
22 E. Blowell. B.C. Storm Fatal to 6; Power Off, The Globe and Mail, 15 Oct 1962, 1.
23 M. Cernetig, Hundreds trapped in cars for 14 hours near Whistler, The Vancouver Sun, 16 Dec 2006, A1.
24 J. Fowlie, Traffic snarled, 190,000 homes without power, The Vancouver Sun, 12 Dec 2006, A1.
25 S. Simpson. Hydro faces 'motherlode' of problems, The Vancouver Sun, 16 Dec 2006, A8.
26 M. Bruneau, S. E. Chang, R. T. Eguchi, G. C. Lee, T. D. O'Rourke, A. M. Reinhorn, M. Shinozuka, K. Tierney, W. A. Wallace and D. von Winterfeldt, A framework to quantitatively assess and enhance the seismic resilience of communities. Earthq. Spectra, 19 (2003) 733-752.
27 US Department of Energy, Emergency Support Function #12, Pacific Northwest Storms Situation Reports, 2007.
28 IEEE Guide for Electric Power Distribution Reliability Indices, IEEE Standard 1366, 2001.
29 R. E. Brown, S. Gupta, R. D. Christie, S. S. Venkata and R. Fletcher, Distribution system reliability assessment: momentary interruptions and storms, IEEE Trans. on Power Delivery, 12 (1997) 1569-1575.
30 D. A. Reed, Electric power distribution system performance for winter storms. J. of Wind Eng. and Ind. Aerodyn., 96 (2008) 123-140.
31 F.G. Hirata, Mapping and Modeling the Probability of Tree-Related Power Outages Using Topographic, Climate and Stand Data, Master's Thesis, University of British Columbia, 2011.
32 B. Taylor and T. Neale, Preliminary Wind Thresholds for Power Outages on Vancouver Island, 4th Annual Canadian Risk and Hazards Network Symposium, Richmond, BC, 06-08 Nov 2007.
33 D. Wilks, Statistical Methods in the Atmospheric Sciences, Academic Press, 1995, pp. 238-248.
34 D. Zhu, D. Cheng, R.P. Broadwater and C. Scirbona, Storm modeling for prediction of power distribution system outages, Elect. Power Syst. Res., 77 (2007) 973-979.
35 H. Liu, R.A. Davidson, T.V. Apanasovich, Spatial generalized linear mixed models of electric power outages due to hurricanes and ice storms, Reliab. Eng. Syst. Saf., 93 (2008) 897-912.
36 Y. Zhou, A. Pahwa, S. Yang, Modeling weather-related failures of overhead distribution lines, Trans. Power Syst., 21 (2006) 2270-2279.

37 S.J. Green, J. Sullivan, C. Clarridge, P. Whitely and R. Tuinstra, Book narrator, four in family among 13 dead, The Seattle Times, 27 Dec 2006.
38 R.K. Gulati, T. Kwan-Gett, N.B. Hampson, A. Baer, D. Shusterman, J.R. Shandro, J.S. Duchin, Carbon monoxide epidemic among immigrant population: King County, Washington, 2006, American J. of Public Health, 99 (2009) 1687-1692.
39 D. Carrigg, Elderly Burnaby couple die of carbon-monoxide poisoning, The Province, 18 Dec 2006, A3.
40 Climate Prediction Center, Monthly U.S. Soil Moisture (mm), Available from: http://www.cpc.ncep.noaa.gov/cgi-bin/US_Soil-Moisture-Monthly.sh, Last accessed 07 May 2013.
41 S. Mitchell, J. Rodney, Proc. of the Windthrow Researchers Workshop, Section 4, Techniques for Reducing Damage, 2001, pp. 204-222.
42 B.R. Christopher R.D. Holtz, Geotextile Engineering Manual, Published by the US Department of Transportation, Federal Highway Administration, Washington, DC, FHWA-TS-86/203, 1985, 1044 pp.
43 F. Krimgold, J. Bigger, M. Willingham and L. Mili, Power Systems, Water, Transportation and Communications Lifeline Interdependencies, Draft report, March 2006, Available from http://www.americanlifelinesalliance.com.
44 M. Gilroy, Severe weather storm hits Puget Sound creating major quality event. Proceedings of the Pacific Northwest Weather Workshop – 2007, University of Washington, Department of Atmospheric Sciences, Seattle, WA, 02-03 Mar 2007.